NEW APPROACH FOR A BEARINGLESS THREE-PHASE INDUCTION MACHINE WITH DIVIDED WINDING

José Álvaro de Paiva[1], Jossana M. S. Ferreira[2], Felipe E. F. Castro[2], Stella N. D. Lisboa[2], Andrés O. Salazar[2] and André L. Maitelli[2]

1 – Centro Federal de Educação Tecnológica do Rio Grande do Norte
Gerência de Informática, Salgado Filho Av., 1559, Natal, RN, Brazil

2 – Universidade Federal do Rio Grande do Norte
Campus Universitário, Departamento de Computação e Automação, Natal, RN, Brazil
josealvaro@cefetrn.br, jossana@dca.ufrn.br, felipeefc@ibest.com.br and stella_lisboa@yahoo.com.br
andres@dca.ufrn.br, maitelli@dca.ufrn.br

ABSTRACT

This paper shows a new approach for a bearingless three-phase induction machine with divided winding. The studies of this machine have evolved significantly, providing a more efficient and compact system. The constructed machine is a four pole 0.25 kW bearingless induction motor. For the system control the DSP (Digital Signal Processor) device is used. The radial positioning is accomplished through the forces control generated by the internal machine fields. The rotor windings were developed to operate with minimum induced currents and to facilitate the electric torque decoupling in relation to the radial positioning control. The system control is a program written in an ANSI C standard language, where two digital PID (Proportional-Integrative-Derivative) controllers are implemented for the radial positioning and six Proportional controllers for the current control. The system uses a state observer for the speed control by PID controller. The used DSP resources are the A/D input channels for the voltages and currents reading, the PWM outputs for the inverters control, the serial RS-232 interface and parallel ports for communication with the PC.

INTRODUCTION

From the late 1980's to early 1990's, some important concepts had been proposed on bearingless machine A general theory of bearingless drives has been introduced [1]. The basic structure is having 4-pole and 2-pole windings in the stator core and the conventional stator machine with divided windings [2,3,4,5]. The motor and radial positioning windings are connected to inverters regulated by a digital controller with an application of vector control theory. Since the middle of 1990's the bearingless machine developments are widely spreading, in special the first technology with some industrial applications[6].

This paper presents the last results over the second technology bearingless machine with divided winding. It is studied a bearingless three-phase induction machine with divided winding [7,8]. The winding configuration and the utilization of only one winding to generate the rotating field and the radial positioning force evolved from the Brazilian bearingless two-phase machine. However, the rotor configuration used is has special winding configuration.

In this project, a three-phase induction machine with divided winding of 4 poles and 0.25kW has been chosen and used. The machine works with high radial forces with the proposed rotor[9,10]. Several tests and researches had been done in order to obtain an optimized four poles winding model. This model minimizes the currents induced in the rotor windings and, consequently, the torque influence in the radial positioning control.

The digital control is carried out by a DSP. The reason of choosing such device as the controller of the system is due to the several potential advantages provided: offers low processing times, several input/output resources and high capacity to execute instructions inside of control loop [11]. The control program was developed in the ANSI C language where the conventional controllers PID (proportional-Integrative-derivative) were implemented for the radial positioning control and proportional for the current control. The DSP facilitates the communication with a PC through the parallel ports and the serial RS-232 interface. Such device provides complementary hardware components as A/D and D/A conversion Channels and PWM output channels responsible in driving the six

inverters and, consequently, feed this specific three-phase Bearingless Induction Machine.

BEARINGLESS INDUCTION MACHINE DESCRIPTION

The configuration of the used bearingless three-phase induction machine windings is nearly similar to a conventional induction machine, as showed in Figure 1. The difference is the division of each phase winding in two parts, which are individually controlled. The machine needs six inverters that control each half winding independently. This way the currents can be controlled to increase the force in a desired direction in order to position the rotor and at simultaneously keeping the torque generation.

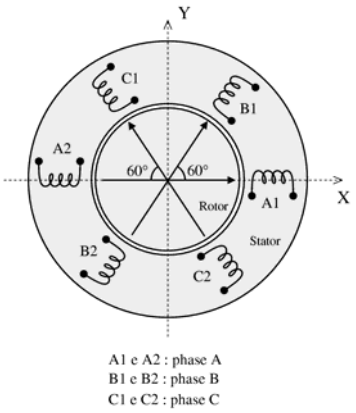

FIGURE 1: Space disposition of the stator windings

The proposed arrangement allows a pondered division of the phase current independently. This way, when there is a rotor displacement in only one direction, the current in the half windings of the same phase will be unequal, increasing on one side and decreasing on the other. In this way, the control acts in a sense to increase the force in the larger air gap direction and decrease on the opposite side, maintaining constant the sums of the current in the winding of the same phase, and keeping the position and the magnitude of the rotating field.

For optimization of the rotor winding, several tests were accomplished by the mean of different windings configurations, where different numbers of wires were inserted, in a way to increase the radial forces [9].

Some specific characteristics of the rotor have brought better concerning the radial force. The rotor is set with twelve circuits, each one creating four-pole magnetic circuit possibilities. This guarantees the existence of only four-pole currents on the rotor, thus eliminating possible interferences. The chosen configuration is presented in the Figure 2.

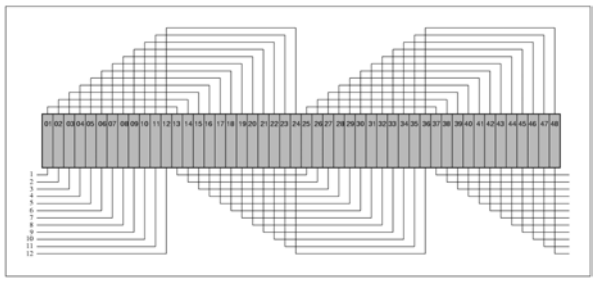

FIGURE 2: Rotor winding model proposed with 12 isolated circuits.

CONTROL SYSTEM IMPLEMENTATION

The control of the machine is divided in three parts: the current control, the radial positioning control and the speed control. For the current control, six proportional controllers were implemented, one for each stator winding. For the radial positioning control two digital PID controllers had been used. The system has a flux and speed estimator, which uses the stator voltages and currents as inputs. The estimated speed is compared with the reference speed and then, the error is compensated by the PID speed controller through the frequency and the flux phase manipulation. The system block diagram is showed in the Figure 3.

For the positioning and current control implementation, the use of a DSP provides a faster and more compact system. The time for control signals acquisition and treatment can reach up 500 ns. The chosen DSP works at 40 MHz and has 12 PWM channels, 16 analog input channels with 10-bits resolution, and 2 interfaces for serial synchronous and asynchronous communication [11]. The DSP can offer in only one device support to all inputs and outputs necessary to the position and current controllers implementation.

The positioning control is based on rotor position measurements performed by two optical sensors, which are arranged in an orthogonal way, where each one is responsible for acquisition of the rotor position in each axis. The sensors send the information to the DSP that, based on reference values, generates the six sinusoidal control signals, which will be the references for the current controllers, which operates with Hall effect sensors measurements. In other words, six of these sensors (one for each stator half winding) support the feedback for the current control loops.

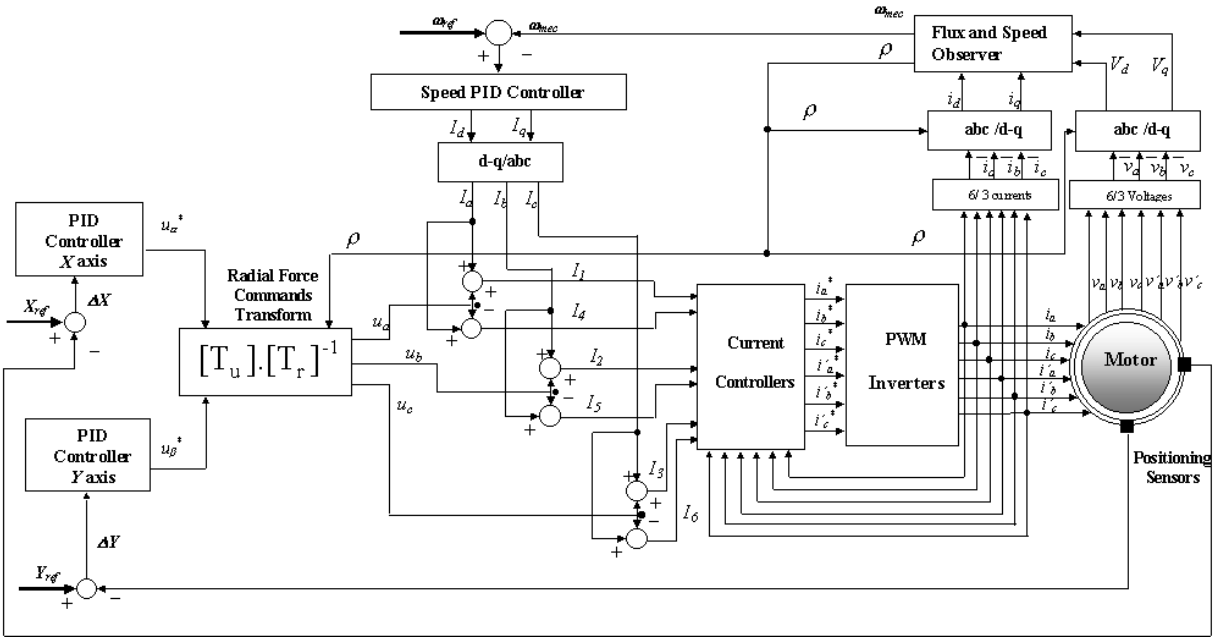

FIGURE 3: Control System Diagram

In order to follow the flux position and to stay synchronized with the speed control, the control actions u_α^* and u_β^* pass by a coordinate transformation, and so generating then, the actions u_a, u_b and u_c. For the radial positioning the modulation is made as showed in the equation 1.

$$\begin{bmatrix} u_a \\ u_b \\ u_c \end{bmatrix} = [\mathrm{T_u}].[\mathrm{T_r}]^{-1}.\begin{bmatrix} u_\alpha^* \\ u_\beta^* \end{bmatrix} \qquad (1)$$

where T_u is a linear transformation matrix and T_r is a rotational transformation matrix.

The sums and subtractions of the control actions u_a , u_b and u_c with the reference currents I_a, I_b and I_c are individually applied in the half windings of each stator phase.

For the phase A, at the same time that the action u_a is added with a current I_a in the half winding, the same action u_a is subtracted in the other half winding, generating a force beside the winding with larger flux, until the reference X_{ref} is reached. In a similar way to the phase A, the respective sums and subtractions of u_b and u_c are applied in the phases B and C for the control on the Y_{ref} direction. The resulting force will be a vectorial composition of the individual forces of each phase.

The equation 2 describes the currents operation in each half winding, whose result is used as reference for the current control.

$$\begin{bmatrix} I_1 \\ I_2 \\ I_3 \\ I_4 \\ I_5 \\ I_6 \end{bmatrix} = \begin{bmatrix} I_a + u_a \\ I_b + u_b \\ I_c + u_c \\ I_a - u_a \\ I_b - u_b \\ I_c - u_c \end{bmatrix} \qquad (2)$$

This transformation in the control signal allows treating the saturation and an eventual abnormal increase of the rotor radial velocity, improving thus the system stability.

THE CONTROL ALGORITHM

The flux diagram showed in the Figure 4 represents the implemented algorithm for the control system. It consists basically of some initial configurations of the system, as well as the configurations of the DSP modules. After the initial settings, the program enters in an infinite loop where the rotation is controlled and the execution of an interruption treatment routine is expected, activated to a frequency of 13,33 kHz. This routine is responsible for the motor positioning and current controls.

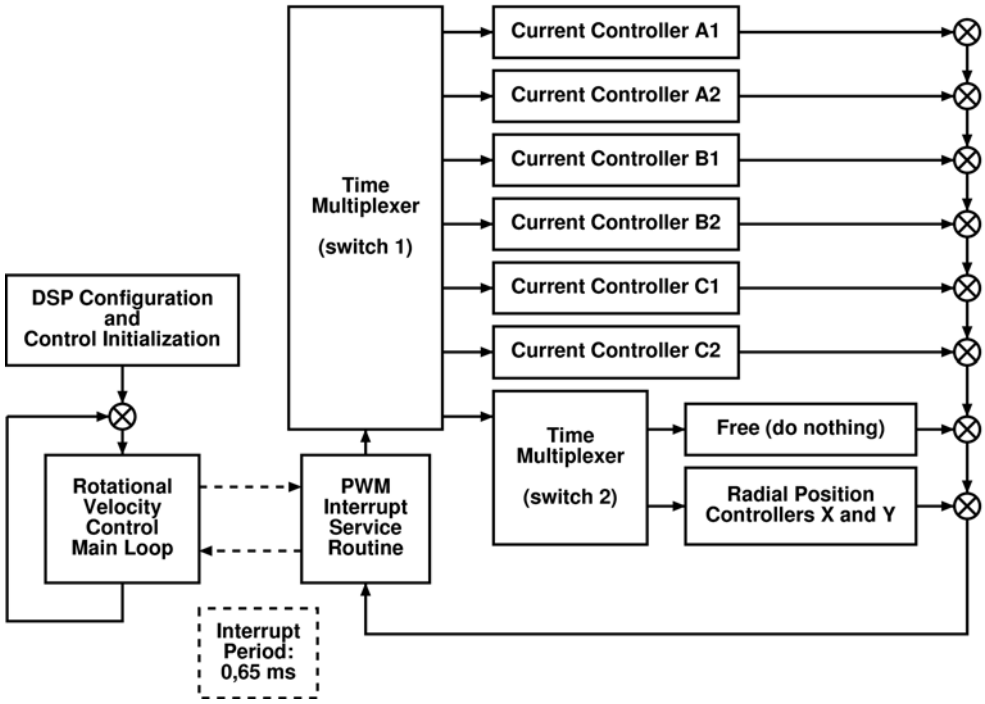

FIGURE 4: General diagram of the control algorithm

EXPERIMENTAL RESULTS

Using some simplifications, two independent models can be obtained for the orthogonal directions of the rotor radial position control. The following equation shows the transfer function relating the radial rotor position in one of the two directions and the force applied over the rotor along that axis.

$$\frac{\text{Position}(s)}{\text{Current}(s)} = G(s)\frac{K_1 I_m}{s^2 - (K_2 I_m)^2} \qquad (3)$$

where K_1 and K_2 are constants that depend on the machine geometry and composition; I_m is the average amplitude of the sinusoidal magnetizing currents imposed through the stator windings. It is observed that the bigger the magnetizing currents get, the more difficult is the control of the plant, because the unstable pole becomes more and more distant from the origin in a zero-pole plot for this system. So, the magnetizing current is a very important parameter for the stabilization, affecting deeply the system dynamics. The derivative action of a PID controller can accomplish the stabilization task. And the integrative part is very useful on mitigating the rotor weight disturbance. The PID parameters that showed the best performance was:

$K_p = 10.13$ (proportional gain)

$K_d = 1.9$ (derivative gain)

$K_i = 0.05$ (integrative gain)

The tests made on the proposed system were accomplished in the nominal operational conditions with load variations.

The figure 5 shows the currents waveforms in two of the six stator windings corresponding to two different phases, both operating under the nominal frequency of 60 Hz.

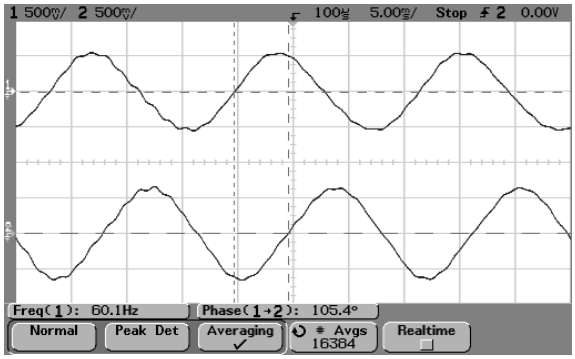

FIGURE 5: Two windings currents of different phases, at 60 Hz – Scale: 1.5 A/Div

The figure 6 shows the sensor signals of radial position on a transverse plan of the machine (X versus Y). The larger circle is the mechanical limit set in a way to avoid the physical contact between the rotor and stator. The central gray stain is the area in which the rotor is confined by the active control and the black trace is a sample of the radial course of the rotor during a short period of time.

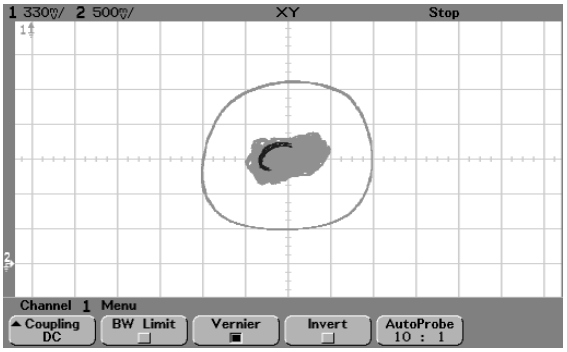

FIGURE 6: Rotor orbit of radial displacement around the central axis for a nominal frequency (60Hz) – Scale: 180 μm/Div

The figure 7 shows the radial forces level that the machine is capable to support along the Y axis, and also of the differential currents existent in the opposite winding, which are necessary to maintain the rotor centralized.

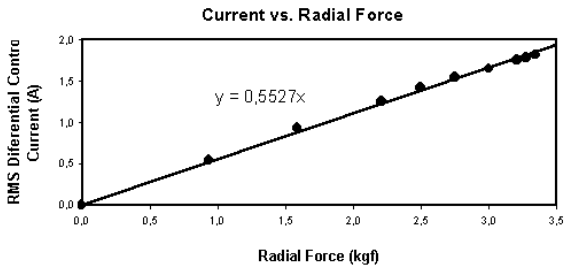

FIGURE 7: Radial Force applied along the Y axis *versus* Current Control

CONCLUSIONS

According to obtained results, it was possible to confirm the high performance of the system, mainly what concerns to the load variation from 0 to 3kgf. This represents an improvement of around ten times, when compared to the first results.

With such improvement, it is now possible to implement a more robust system for the bearingless machine control.

An important result is the independent control of the radial forces in relation to the electric torque of the machine. This specific control was obtained through the generation of minimum induced currents.

In order to reduce the implementation costs, a speed observer is being developed. This observer is based on the conventional methods of the state estimation. To turn the system more robust to parametric variations and the machine non-linearities, in a near future, artificial intelligence techniques, such as Neural Networks or Fuzzy controllers, will be applied.

After the conclusion of the system development, the control strategy will be then applied to a horizontal machine of 1kW with two motor-bearing sets and based on the same characteristics of the first vertical prototype.

REFERENCES

[1] A. Chiba, K. Chida and T. Fukao, “Principle and characteristics of a reluctance motor with windings of magnetic bearing”, IPEC, Japan, pp.919-926, Apr. 1990.

[2] A.O. Salazar, W. Dunford, R. Stephan, E. Watanabe, “A magnetic bearing system using capacitive sensors for position measurement”, IEEE Trans. on Magnetics, Vol.26 No.5, pp.2541-2543, Sept. 1990.

[3] A. O. Salazar, R.M. Stephan, W. Dunford, “An efficient bearingless induction machine”, COBEP, pp.419 - 424, Brazil, 1993.

[4] A. O. Salazar, R. M. Stephan, “A bearingless method for induction machine”, IEEE Trans. On Magn., Vol.29, No. 6, pp 2965-2967, Nov. 1993.

[5] T. Gempp, R. Schob, “Design of a bearingless canned motor pump”, ISMB, pp 333-338, Kanazawa, Japan, 1996.

[6] K.B. Yahia, G. Henneberger, “Development of bearingless induction motor”, MOVIC, Zurich, Switzerland, Vol. 3, pp 1083-1087, Aug. 1998.

[7] J. M. S.Ferreira, “Proposta de máquinas de indução trifásica sem mancal com bobinado dividido” – Dissertação de mestrado, 63p.: il. Natal, 2002.

[8] Y. Okada, K. Shinohara, S. Ueno and T. Ohishi, “ hybrid AMB type self bearing motor”, Int. Symp. Magnetic Bearing, pp. 497-506, 1998.

[9] A Chiba, T. Fukao, "Optimal design of rotor circuits in induction type bearingless motors", IEEE Trans. on Mag, Vol.34, No.4, (1998).

[10] J. A. Santisteban, D. F. B. David, R. M. Stephan, Arthur Ripper, R. de A. Jr., A. S. Pereira, R. Nicolsky, “Hybrid bearing for induction machine with controlled electromagnetic positioning and superconducting levitation”, Inter., Magnetics Conference, Canada, Apr. 2000.

[11] TMS320LF2407A manual of Texas Instruments Inc®.